

1
2
3
4
5
6
7
8
9
10
11
12
13
14
15
16
17
18
19
20
21
22
23
24
25

Supplementary Materials for

European plants lagging behind climate change pay a climatic debt in the North, but are favored in the South

François Duchenne, Gabrielle Martin & Emmanuelle Porcher

Correspondence to: francois.duchenne@mnhn.fr

This PDF file includes:

Supplementary Methods
Figure S1 to S9
Caption for Table S1
Table S2 & S3

Other Supplementary Materials for this manuscript include the following:

Table S1

26 **Supplementary Methods:**

27 *DOIs*

28 For computational reasons we split the extractions from the GBIF into 10 parts, accessible
29 through the 10 followings DOI:

30 GBIF.org (01 May 2020) GBIF Occurrence Download <https://doi.org/10.15468/dl.z8kcad>

31 GBIF.org (01 May 2020) GBIF Occurrence Download <https://doi.org/10.15468/dl.fyakne>

32 GBIF.org (01 May 2020) GBIF Occurrence Download <https://doi.org/10.15468/dl.7u7dgx>

33 GBIF.org (01 May 2020) GBIF Occurrence Download <https://doi.org/10.15468/dl.ske4qr>

34 GBIF.org (01 May 2020) GBIF Occurrence Download <https://doi.org/10.15468/dl.bhfw37>

35 GBIF.org (01 May 2020) GBIF Occurrence Download <https://doi.org/10.15468/dl.zy2nhr>

36 GBIF.org (01 May 2020) GBIF Occurrence Download <https://doi.org/10.15468/dl.67dgze>

37 GBIF.org (30 April 2020) GBIF Occurrence Download <https://doi.org/10.15468/dl.3b8bc8>

38 GBIF.org (30 April 2020) GBIF Occurrence Download <https://doi.org/10.15468/dl.p5awfb>

39 GBIF.org (30 April 2020) GBIF Occurrence Download <https://doi.org/10.15468/dl.kjv523>

40 *Plant species selection*

41 We removed crop and ornamental species from this list, using an FAO reference list for
42 crop species

43 (http://www.fao.org/fileadmin/templates/ess/documents/world_census_of_agriculture/appendix4_r7.pdf) complemented by visual inspection of the list. We also considered invasive species

45 separately; they were identified using the European Union list for invasive species

46 (https://ec.europa.eu/environment/nature/invasivealien/index_en.htm), complemented by

47 visual inspection. By definition, invasive species have increased in abundance/occupancy in the

48 recent past; this allowed us to check that occupancy trends as calculated below were able to
49 detect these increases (Fig. S3).

50 To homogenize taxonomy among these lists and our dataset, we used the GBIF backbone
51 taxonomy, which is designed to avoid synonymy issues among datasets, all along the paper.

52 *Potential drivers of occupancy trends*

53 For each species, we calculated historical climatic indices for the six bioclimatic variables
54 studied here. To do so, we averaged SCIs over 1951-1980 (i.e. stopping before the recent sharp
55 temperature increase, Fig. S1a) for each species, weighting each year by the number of records
56 of the given species.

57 For nutrient (reflecting mainly nitrophily) and moisture preferences we used the Ellenberg
58 Indicator Values (EIV) from France (Julve 1998), United-Kingdom (Fitter & Peat 1994), Italy
59 (Pignatti *et al.* 2005), Czech Republic (Chytrý *et al.* 2018) and Germany (Ellenberg *et al.* 1992).
60 All EIVs are on the same scale, but they are a relative measure of species preference, depending
61 on the species assemblages used. As these species assemblages depend on the source, a given
62 value can reflect distinct nutrient/moisture preferences among sources. Using species shared
63 across EIV sources, we corrected biases among data sources, using the following formula:

$$64 \quad EIV_{x_s}' = EIV_{x_s} + \frac{\sum_{j=1}^n EIV_{Baseflor_j} - EIV_{x_j}}{n} \quad (5)$$

65 where EIV_{x_s} is the Ellenberg indicator value of species s in source x and n the number of
66 species shared between the source x and Baseflor, which was used as a reference because it
67 contains information for the largest number of species. Finally, for species present in several
68 data sources we used the average corrected EIVs, over all sources. The whole procedure was
69 performed independently for moisture and nutrient preferences.

70 Pollen vector (i.e. insects, wind or self-fertilization) was retrieved from the Baseflor (Julve
71 1998), Ecoflora (Fitter & Peat 1994) and BiolFlor (Kühn *et al.* 2004) databases. Many species
72 are associated with several types of pollen vectors, both within and among databases. We
73 encapsulated this variability into a single variable: pollinator dependency, the percentage of
74 times “insects” appear as a pollen vector for a given species, across all databases. Pollinator
75 dependency ranges from 0, for species that are never associated with insect pollination in the
76 trait databases and that should be therefore independent of pollinators for their reproduction, to
77 100, for species that are only associated with insect pollination, and that should be strictly
78 dependent on pollinators for their reproduction.

79 The lifespan of each species was extracted using the R package *TR8* (Gionata 2015) from
80 BiolFlor and LEDA (Kleyer *et al.* 2008) databases and coded following Martin *et al.*'s (2019)
81 categories but with three levels only: strict annual plants, intermediate plants (biennial,
82 annual/perennial, etc.) and strict perennial plants.

83 Habitat affinity was calculated following the same principles as for SCIs, but averaged over
84 the whole time period (1951-2014). We used the EUNIS habitat classification (Davies *et al.*
85 2004) at the first level, but merging all aquatic, wetland and coastal habitats together (Table
86 S2). As for SCIs and occupancy calculation we used a 10km×10km grid cell. In general, the
87 finest spatial resolution is best to calculate species habitat affinity or detect changes in
88 occupancy or species climatic indices. Hence, we chose to limit spatial aggregation as much as
89 possible, but we were constrained first by computation times and second, more importantly, by
90 the spatial resolution of GBIF data: we discarded a spatial aggregation at 1km² because GBIF
91 datasets are often defined at 5 or 10km². For each 10km×10km grid cell, we calculated the
92 percentage of area covered by each habitat. Then, for each species and each habitat, we
93 calculated the weighted mean of the habitat coverage over the range of each plant species,
94 weighting the contribution of each cell (10×10km²) by the ratio of the number of records of this

95 species on the number for records for all plant species. For each species, we therefore obtained
96 7 habitat affinity indices, each ranging from 0 to 1 and summing to 1 across habitats. They
97 correspond to the fraction of a given habitat in the species distribution.

98 Species traits, SCI and occupancy trends are available in Table S1.

99 *Phylogenetic signal in SCI and occupancy trends*

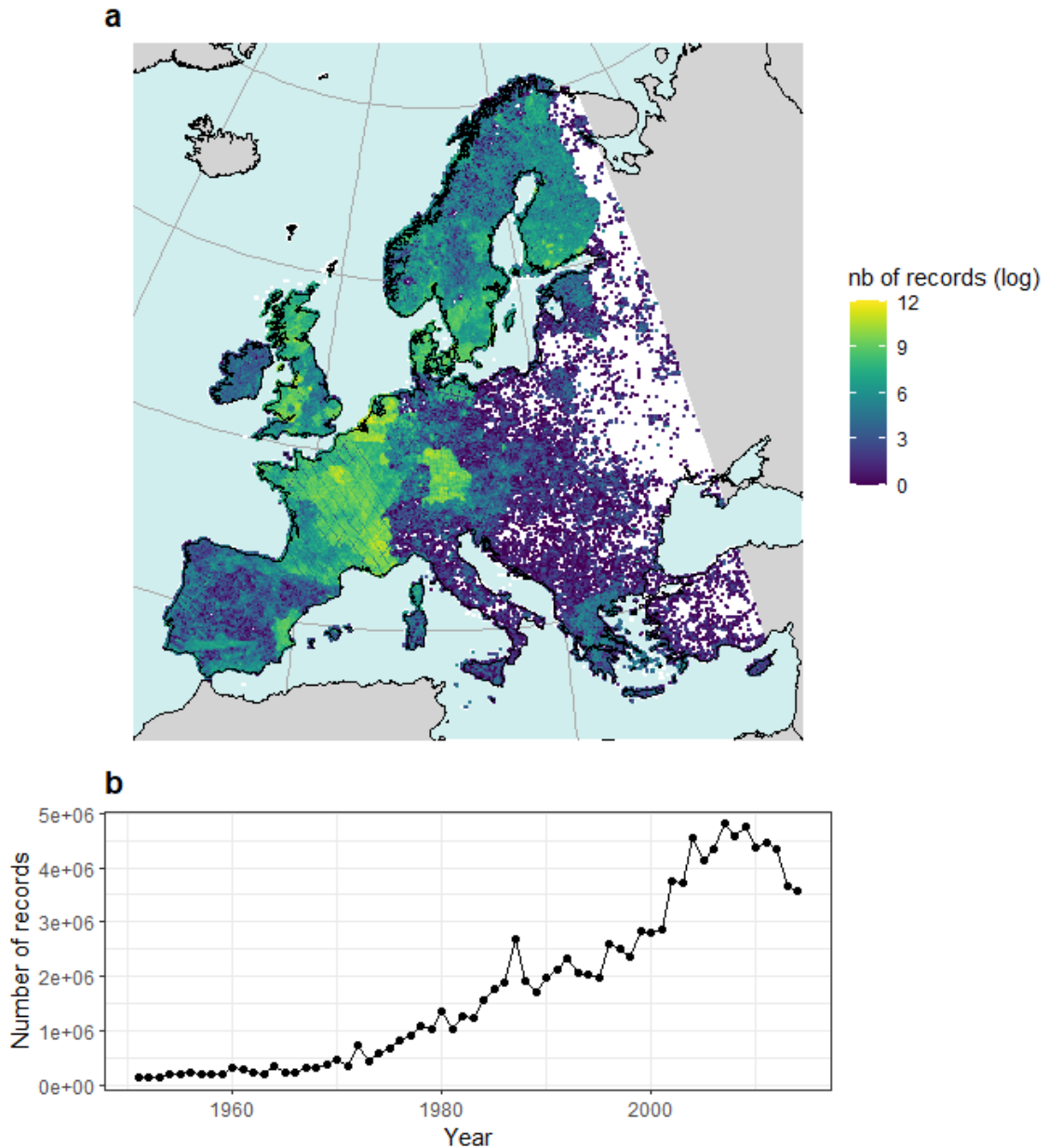
100 Estimating phylogenetic signal in species response informs us on plausible evolutionary
101 constraints on mechanisms underlying SCI and occupancy trends. To analyze the phylogenetic
102 structure of SCI and occupancy trends, we used the *Daphne* phylogeny of European flora
103 (Durka & Michalski 2012). Of the 4,120 species we analyzed, 1,335 were not included in the
104 phylogeny, thus we excluded them for phylogenetic analysis, and focused on the 2,785
105 remaining species. We assessed the phylogenetic structure using Pagel's λ , implemented in the
106 *phylosignal* R package (Keck *et al.* 2016), and tested its significance by randomizing the tips
107 of the phylogeny 1,000 times, for both SCI and occupancy trends.

108 *Evidencing the role of the recent climatic change in observed effects*

109 To confirm that the costs of the shifts in experienced climatic conditions occur only after
110 the acceleration of climate change (1980-2000, Fig. S5), we performed the same set of analyses
111 on the earliest data, taking the first 40 years (1951-1990), i.e. including 1980-1990 to retain
112 enough records and years to estimate SCI and occupancy trends. We calculated SCI trends and
113 occupancy trends between 1951 and 1990. For SCI trends, we used only records from 1951 to
114 1990. For occupancy trends, we used all records and the same model as in equation (2) but with
115 a broken-line model for the year effect, as implemented in the *segmented* R package (Muggeo
116 2008), with a breakpoint in 1990. Such method enables estimation of random site effects and
117 effect of the species list length on the entire dataset while modelling a trend for 1951-1990.
118 Results are shown in Fig. S6.

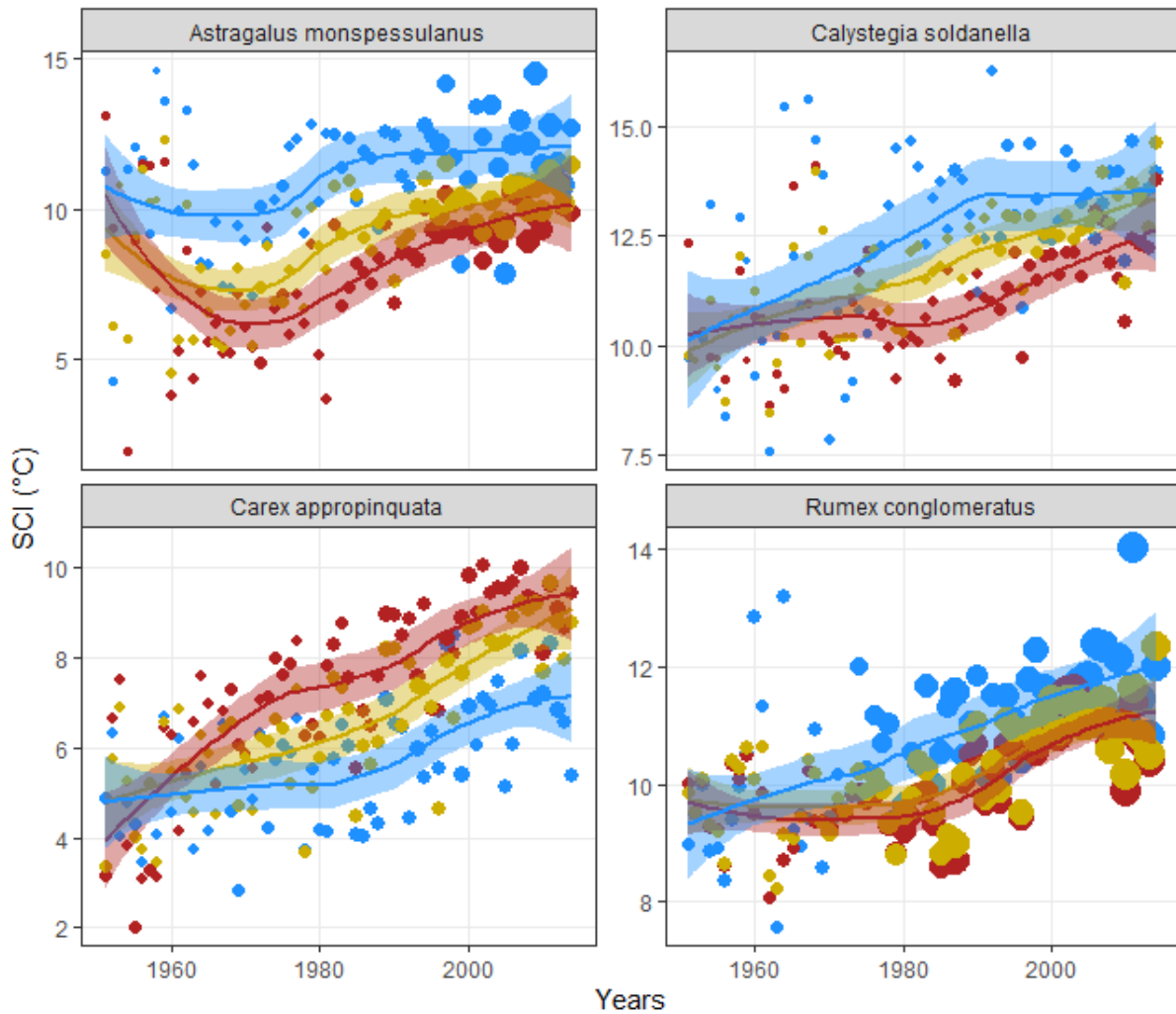
119 References

- 120 Chytrý, M., Tichý, L., Dřevojan, P., Sádlo, J. & Zelený, D. (2018). Ellenberg-type indicator
121 values for the Czech flora. *Preslia*, 90, 83–103.
- 122 Davies, C.E., Moss, D. & Hill, M.O. (2004). EUNIS habitat classification revised 2004, 310.
- 123 Durka, W. & Michalski, S.G. (2012). Daphne: a dated phylogeny of a large European flora for
124 phylogenetically informed ecological analyses. *Ecology*, 93, 2297–2297.
- 125 Ellenberg, H., Weber, H.E., Düll, R., Wirth, V., Werner, W., Paulißen, D., *et al.* (1992).
126 Zeigerwerte von pflanzen in Mitteleuropa.
- 127 Fitter, A.H. & Peat, H.J. (1994). The Ecological Flora Database. *J. Ecol.*, 82, 415–425.
- 128 Gionata, B. (2015). TR8: an R package for easily retrieving plant species traits. *Methods Ecol.*
129 *Evol.*, 6, 347–350.
- 130 Julve, P. (1998). Baseflor. Index botanique, écologique et chorologique de la flore de France.
131 *Inst. Cathol. Lille Lille*.
- 132 Keck, F., Rimet, F., Bouchez, A. & Franc, A. (2016). phylosignal: an R package to measure,
133 test, and explore the phylogenetic signal. *Ecol. Evol.*, 6, 2774–2780.
- 134 Kleyer, M., Bekker, R.M., Knevel, I.C., Bakker, J.P., Thompson, K., Sonnenschein, M., *et al.*
135 (2008). The LEDA Traitbase: a database of life-history traits of the Northwest European
136 flora. *J. Ecol.*, 96, 1266–1274.
- 137 Kühn, I., Durka, W. & Klotz, S. (2004). BioFlor — a new plant-trait database as a tool for
138 plant invasion ecology. *Divers. Distrib.*, 10, 363–365.
- 139 Muggeo, V.M.R. (2008). segmented: an R Package to Fit Regression Models with Broken-Line
140 Relationships. *R News*, 8, 20–25.
- 141 Pignatti, S., Menegoni, P. & Pietrosanti, S. (2005). Indicazione attraverso le piante vascolari.
142 Valori di indicazione secondo Ellenberg (Zeigerwerte) per le specie della Flora d’Italia.
143 *Braun-Blanquetia*, 3, 91–97.
- 144

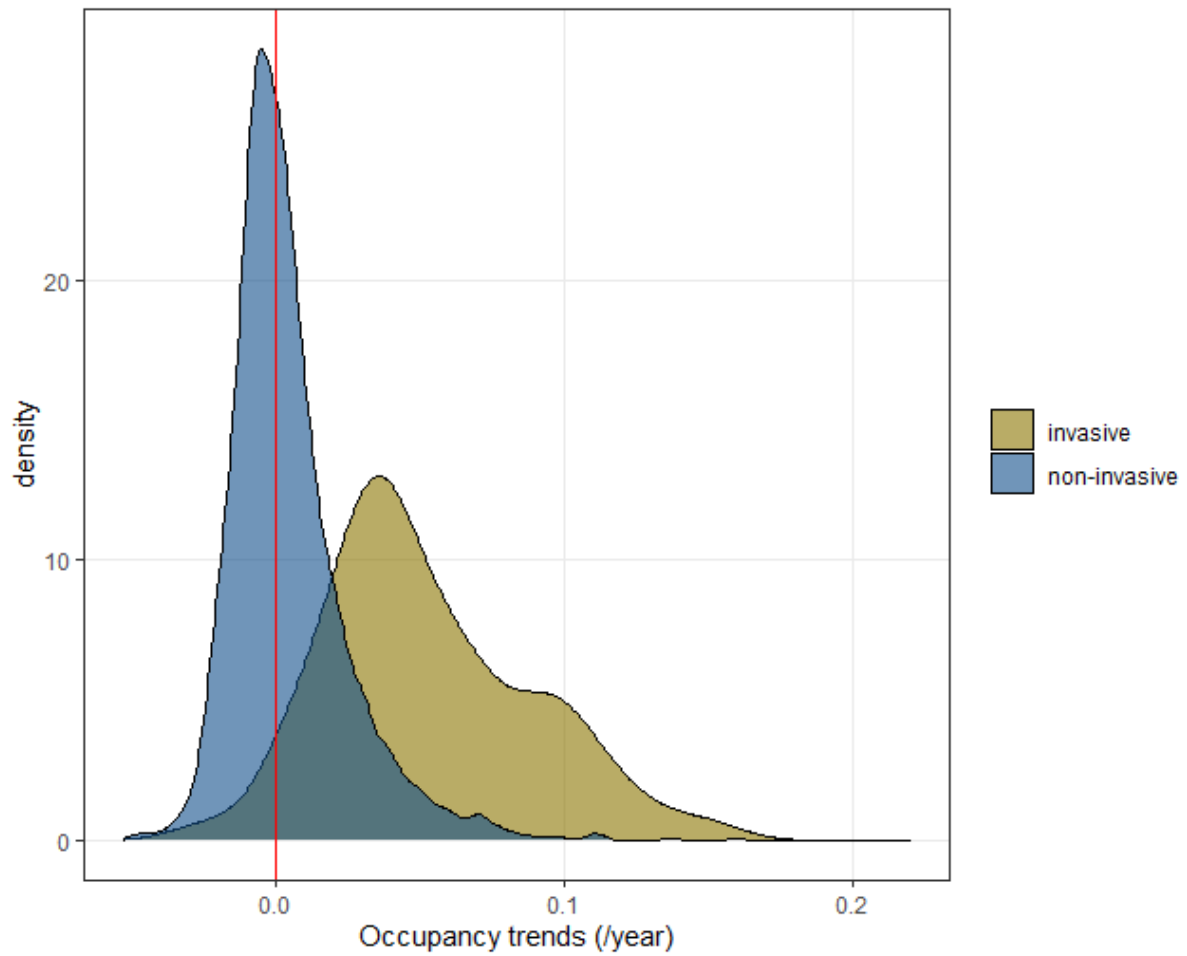


145
 146
 147
 148
 149
 150
 151
 152
 153
 154
 155
 156

Figure S1: Spatial and temporal distribution of the records used. (a) Spatial distribution of the records used, grouped by $\sim 100\text{km}^2$ grid cells. White grid cells correspond to cells with no data and grey cells are outside of the study area. Hexagonal patterns in France are due to the main data source from France (CBN dataset: <https://www.gbif.org/fr/dataset/75956ee6-1a2b-4fa3-b3e8-ccda64ce6c2d>). This dataset was aggregated spatially using WSG84 coordinates, leading to grid cells with heterogeneous area on a map projection. Here we re-projected the entire dataset using grid cells with the same area across Europe. The superimposition of two grids that are not orthogonal, because of distinct projections, led to such periodic patterns. (b) Number of annual records through time, showing a continuous geometric increase over years in the number of data points.

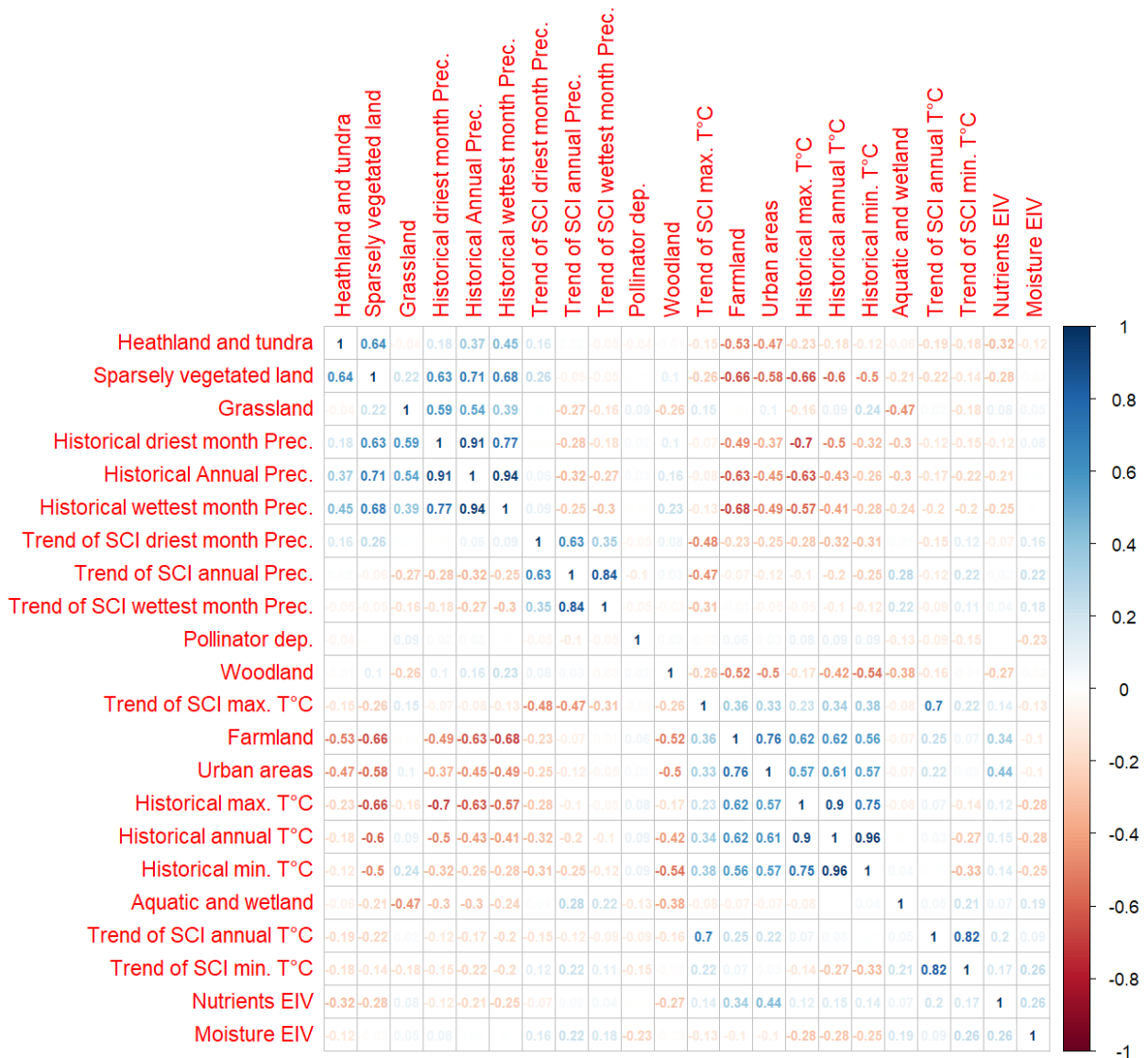


157
 158 **Figure S2:** *Examples of interannual variability in SCIs, using annual mean temperature.*
 159 *SCIs represented by blue points are those used in the paper. They are calculated with a mean*
 160 *weighted by the ratio $\frac{N_{ijk}}{\sum_{s=1}^{nsp} N_{sjk}}$ where N_{ijk} is the number of record of species i , grid cell k and*
 161 *year j . $\sum_{s=1}^{nsp} N_{sjk}$ is the total number of records over all plant species for a given year and grid*
 162 *cell. SCIs represented by yellow points are calculated with a mean weighted by N_{ijk} , which*
 163 *accounts for sampling pressure (represented by $\sum_{s=1}^{nsp} N_{sjk}$). The red curve is the mean weighted*
 164 *by $\begin{cases} 1 & \text{if } N_{ijk} > 0 \\ 0 & \text{if } N_{ijk} = 0 \end{cases} \times \sum_{s=1}^{nsp} N_{sjk}$, which represents variation in temperature but also temporal bias*
 165 *in the sampling pressure over the geographic range of species i . Circle size is proportional to*
 166 *the number of grid cells included in the (weighted) mean. Curves are the results of locally*
 167 *estimated scatterplot smoothing regressions implemented in ggplot2.*

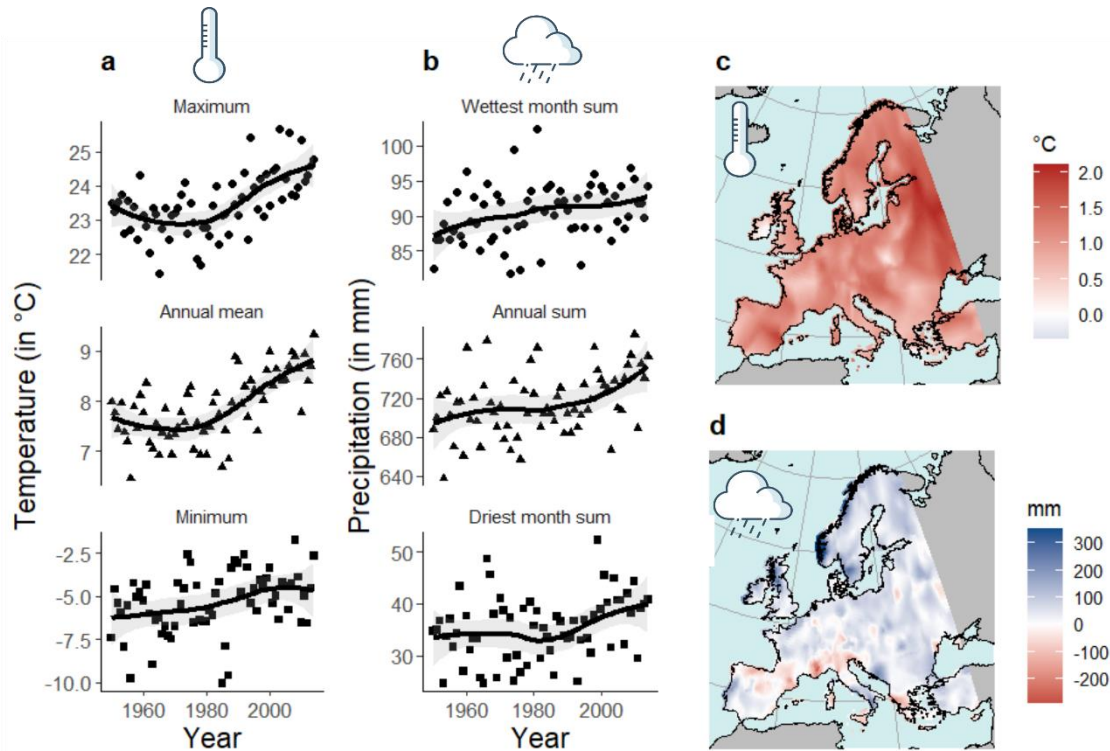


168
169
170
171
172
173

Figure S3: Occupancy trends of non-invasive vs. invasive species. Density distribution of occupancy trends for the 4,120 native or naturalized (“non-invasive”) species and for the 58 species that were identified as “invasive” in the species selection. The red vertical line indicates zero.



174 **Figure S4: Correlation matrix among variables potentially added to phylogenetic regression**
 175 **and linear mixed-effect models. The red to blue color ramp represents the sign and strength**
 176 **of the correlation. Variables are ordered in the matrix so that highly correlated variables are**
 177 **clustered.**



179

180

181

182

183

184

185

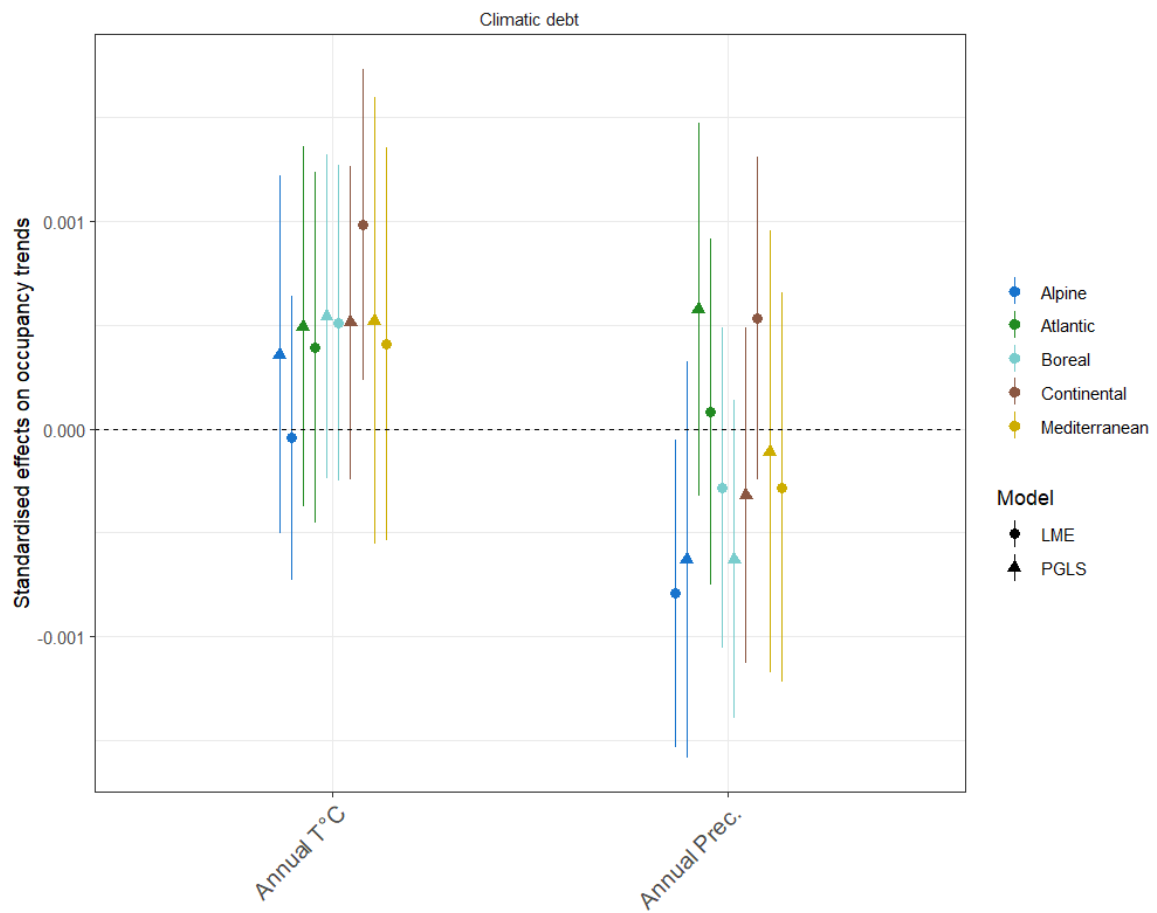
186

187

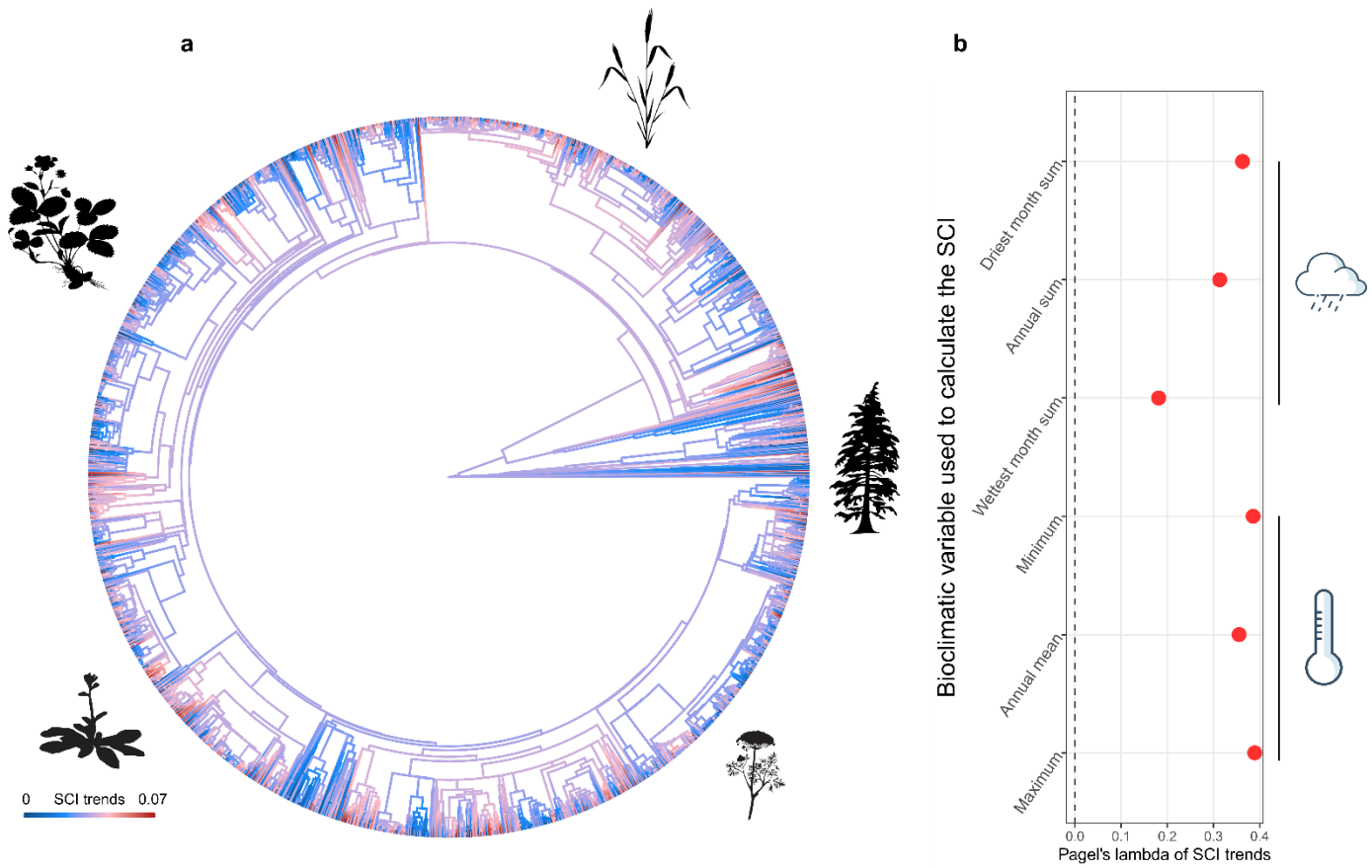
188

189

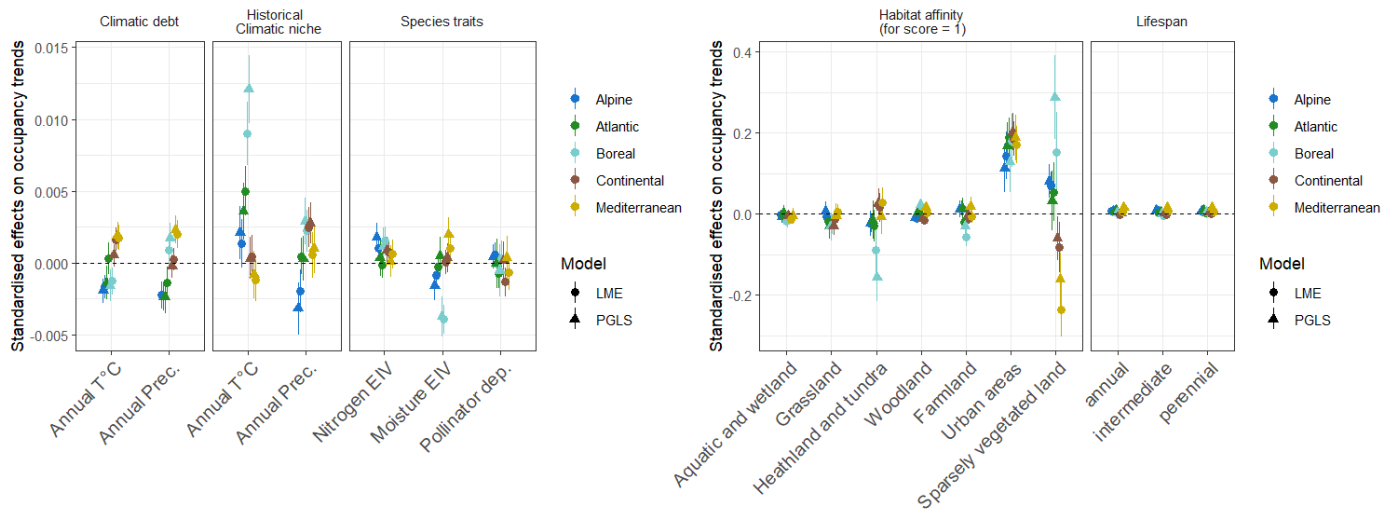
Figure S5: Change in bioclimatic variables across time and space. (a) and (b) show temporal variations in temperature and precipitation respectively, averaged over the study area. Circles depict maximum temperature or precipitation of the wettest month (bio5 & 13), triangles annual mean temperature or annual precipitation (bio1 & 12), and squares minimum temperature or precipitation of the driest month (bio6 & 14). The black lines correspond to LOESS (Locally Estimated Scatterplot Smoothing) curves obtained from the ggplot2 library in R. (c) and (d) illustrate the spatial variation in temporal changes of annual mean temperature and precipitation respectively. Temporal changes were measured here as the difference between the 1950-1960 average and the 2004-2014 average. In (d) the upper bound of the color scale is truncated to 350mm instead of 575mm to preserve readability.



190
 191 **Figure S6: Correlations between occupancy trends and SCI trends from 1951 through 1990.**
 192 *Estimates (\pm CI_{95%}) from phylogenetic regressions (PGLS) and linear mixed-effect models*
 193 *(LME) explaining occupancy trends with temporal trends in SCIs and other species traits.*
 194



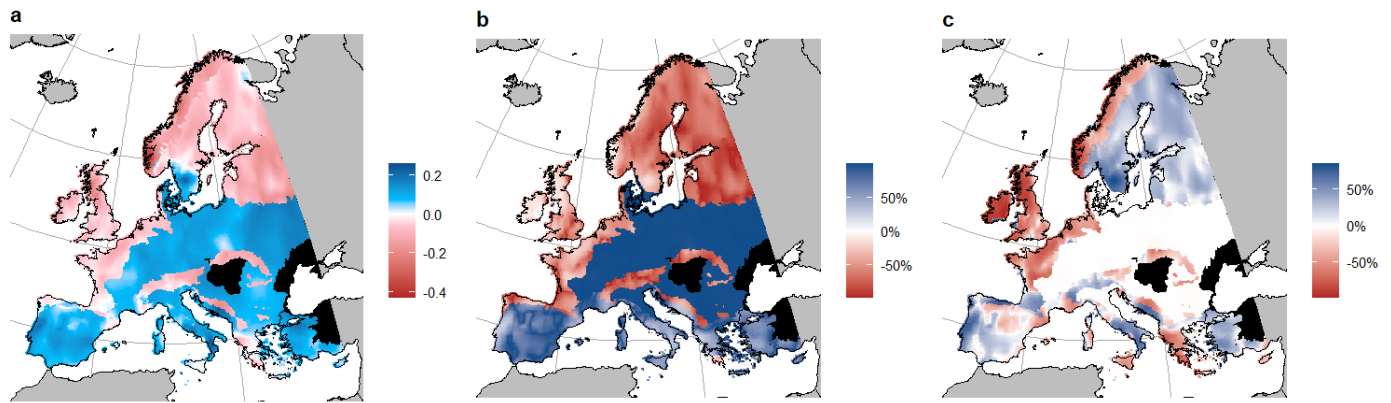
195 **Figure S7: Phylogenetic signal in the linear trends in species climatic indices (SCIs) for the**
 196 **2,785 species included in the phylogeny.** (a) Phylogenetic signal in the SCI trends related to
 197 the annual mean temperature bioclimatic variable (bio1). The color scale is bounded between
 198 the 5th and 95th quantile to preserve readability. (b) Pagel's λ for SCI trends related to the six
 199 bioclimatic variables. Zero (dashed black line) indicates an absence of phylogenetic signal.
 200 Red circles correspond to a significant phylogenetic signal (p -value < 0.05, calculated from
 201 1000 randomizations).
 202



203 **Figure S8: Correlates of occupancy trends for each biogeographic region.** The three left
 204 panels represent the estimates ($\pm CI_{95\%}$) from phylogenetic regression (PGLS) and linear mixed-
 205 effects model (LME), explaining occupancy trends with temporal trends in species climatic
 206 indices (SCIs) and other species traits. The two right panels show predicted averaged
 207 occupancy trends ($\pm CI_{95\%}$) for each habitat, considering a theoretical perfect affinity to each
 208 habitat (score = 1 & lifespan = annual), and for lifespan categories, predicted at the average
 209 of all other variables.

210

211



212 ***Figure S9: Climatic debt/bonus in Europe and its climatic drivers, considering non-***
213 ***significant predictors. Same figure as Figure 4 of the paper but also including the effects of***
214 ***trends in species climatic indices (SCIs) that are not significant. (a) Climatic debt/bonus***
215 ***averaged over all species over the last 65 years. The gradient from white to red indicates a***
216 ***climatic debt (cost of climate change in terms of species occupancy), while the gradient from***
217 ***white to blue indicates a climatic bonus (benefits of climate change in terms of species***
218 ***occupancy); white represents no cost on average for plants. Relative contribution of (b)***
219 ***temperature and (c) precipitation SCI trends to the climatic debt, in percentage. Black regions***
220 ***are biogeographic regions with too few data. The maps were generated using predictions***
221 ***averaged over the linear mixed-effects model (LME) and the phylogenetic regression (PGLS).***

222 **Table S1 (separate file):**
 223 SCI, occupancy trends and species traits for the 4,120 species studied + the 58 invasive
 224 species present in the initial species list.

225
 226
 227
 228
 229
 230
 231
 232

Table S2: EUNIS habitat classification, and the grouped habitat classification used in the study.

EUNIS categories	Our categories
A - Marine habitats	Aquatic and wetland
B - Coastal habitats	Aquatic and wetland
C - Inland surface waters	Aquatic and wetland
D - Mires, bogs and fens	Aquatic and wetland
E - Grasslands and land dominated by forbs, mosses or lichens	Grassland
F - Heathland, scrub and tundra	Heathland and tundra
G - Woodland, forest and other wooded land	Woodland
H - Inland unvegetated or sparsely vegetated habitats	Sparsely vegetated land
I - Arable land and market gardens	Farmland
J - constructed, industrial and other artificial habitats	Urban areas

233
 234
 235
 236
 237

Table S3: Mean and associated CI_{95%} for SCI trends over the 4,120 studied species.

Variable	upper CI95%	Mean	lower CI95%
Annual mean Temperature (bio1)	0.03290744	0.032226788	0.0315461347
Maximum Temperature (bio5)	0.04568614	0.044922632	0.0441591201
Minimum Temperature (bio6)	0.03366092	0.032643692	0.0316264601
Annual Precipitation (bio12)	0.27474310	0.202730377	0.1307176590
Wettest month Precipitation (bio13)	0.01677690	0.008501243	0.0002255894
Driest month Precipitation (bio14)	0.12556774	0.118927077	0.1122864159

238